J. Fluid Mech. (1988), *vol.* 187, *pp.* 487–506
Printed in Great Britain

Upstream motions in stratified flow

By I. P. CASTRO
Mechanical Engineering Department, University of Surrey, Guildford, UK

AND W. H. SNYDER †
Meteorology and Assessment Division, Atmospheric Sciences Research Laboratory, US Environmental Protection Agency, Research Triangle Park, NC 27711, USA

(Received 20 May 1986 and in revised form 5 August 1987)

In this paper experimental measurements of the time-dependent velocity and density perturbations upstream of obstacles towed through linearly stratified fluid are presented. Attention is concentrated on two-dimensional obstacles which generate turbulent separated wakes at Froude numbers, based on velocity and body height, of less than 0.5. The form of the upstream columnar modes is shown to be largely that of first-order unattenuating disturbances, which have little resemblance to the perturbations described by small-obstacle-height theories. For two-dimensional obstacles the disturbances are similar to those found by Wei, Kao & Pao (1975) and it is shown that provided a suitable obstacle drag coefficient is specified, the lowest-order modes (at least) are quantitatively consistent with the results of the Oseen inviscid model.

Discussion of some results of similar measurements upstream of three-dimensional obstacles, the importance of towing tank endwalls and the relevance of the Foster & Saffman (1970) theory for the limit of zero Froude number is also included.

1. Introduction

It is well known that the subcritical flow of a stratified fluid past an obstacle generates motions upstream of the obstacle. Subcritical flow is here defined as a flow for which the Froude number based on channel height is less than $1/\pi$, so that one or more stationary lee waves are present. Some of the upstream motions do not decay with distance upstream. These so-called 'columnar' modes have zero frequency and a sinusoidal structure in the direction of the density gradient; they effectively lead to a continuous change in upstream conditions. If the obstacle is two-dimensional (i.e. of infinite extent in the direction perpendicular to the upstream flow and the direction of density gradient), inviscid theories show that the length of the upstream region affected by the columnar modes increases without bound as $t \to \infty$. Non-zero viscosity (and/or diffusivity) will, however, limit the region affected, since the wave amplitudes will then slowly decay.

There has been considerable discussion in the literature concerning the origin and nature of these disturbances. The inviscid Oseen model, in which the equations for a Boussinesq fluid are linearized and solved as an initial-value problem, has been particularly useful. Trustrum (1964, 1971), Wong & Kao (1970) and Janowitz (1981, 1984) all describe the time-dependent nature of the upstream flow using models of

† On assignment from the National Oceanic and Atmospheric Administration, US Department of Commerce.

this sort. For an upstream flow velocity (or towing speed) of U, a channel depth of D and a linear density gradient with Brunt–Väisälä frequency defined by

$$N = \left(\frac{g}{\rho_0}\frac{\mathrm{d}\rho}{\mathrm{d}z}\right)^{\frac{1}{2}},$$

internal gravity waves can propagate upstream when $\pi U/ND < 1$. With $K = ND/\pi U$, if $n < K$ then n modes will propagate upstream at speeds given by KU/n. Since these modes will eventually distort the conditions far upstream, this is one of the features of confined subcritical flows that makes the exact solutions found by Long (1953, 1955) for finite-amplitude motions inappropriate.

Janowitz (1968) included the viscous terms in his steady-state analysis of finite-amplitude shear waves. He defined a lengthscale $l = (U\nu/N^2)^{\frac{1}{3}}$ and showed that the asymptotic solution for distances (x) far upstream is valid for $x/l \gg Re_l^2$, where $Re_l = Ul/\nu$. Laboratory experiments on upstream influence are often done in tanks where the obstacle is towed through the fluid. Typically, Re_l can then be $O(100)$ and L/l is often $O(10^4)$ (for $U = 5$ cm/s, $N = 1\ \mathrm{s}^{-1}$ and L, the length of the tank, $= 10$ m). Viscous effects are therefore often likely to be important in such experiments, even if a steady upstream state is achieved. Furthermore, in towing-tank experiments the effects of the endwalls cannot always be neglected. Foster & Saffman (1970) studied what happens in the limit of zero Froude number and vanishing viscous diffusion when a body of height h is towed through a linearly stratified fluid in a tank of finite length. They showed quantitatively how the upstream (and downstream) density field changes with time in the region bounded by the horizontal planes through the top and bottom edges of the obstacle – a direct result of the incompressibility condition and the presence of the endwalls. Snyder *et al.* (1985) have referred to this phenomenon as 'squashing'. It arises essentially because of the endwall reflections of the density perturbations produced by the columnar wave modes. In practice, a density discontinuity at $z = \frac{1}{2}h$ cannot occur, because of viscous diffusion, and Foster & Saffman showed that there will certainly be a shear layer whose thickness, δ, is of order $(UhL\nu/N^2)^{\frac{1}{5}}$. In terms of a Froude number and Reynolds number based on *body* height, $\delta/h = (F_h^2\,(L/h)/Re_h)^{\frac{1}{5}}$. In a typical experiment $Re_h = 2000$, $F_h = 0.2$ and $L/h = 100$, so that $\delta/h = 0.3$ and viscous effects will generally be significant.

In addition, viscous effects ensure that the blocked fluid region extends only a finite distance ahead of the obstacle. However, as Tritton (1977, p. 188) has shown, the length of the blocked region can be very large indeed – of order $Re\ h/F_h^2$. For example, with $Re = 2000$, $F_h = 0.2$ and $h = 10$ cm, this corresponds to 5 km! Longitudinal diffusion effects will therefore seldom be significant in towing-tank experiments.

There seems to have been little study of the importance of the 'squashing' effect in towing-tank experiments and, indeed, only recently has any detailed attempt been made to compare experimentally determined upstream velocity and density perturbations with the predictions of even the inviscid Oseen model (Janowitz 1984). In a number of papers, Baines (e.g. 1977, 1979) has studied the upstream disturbances – principally in order to check the validity, for subcritical flows, of Long's model (1955). Generally the disturbances some distance upstream did not seem like those predicted by the Oseen theories. Neither did they have the features of the perturbations that arise in 'small-obstacle-height' theories (as McIntyre's 1972; this is strictly a 'weakly nonlinear' theory). Indeed, McIntyre's theory only predicts second-order perturbations in the steady state and these do not include mode-one ($n = 1$) disturbances at all; these were clearly present in Baines'

experiments. Baines & Grimshaw (1979) have presented an alternative perturbation theory in which the small parameter was taken as the obstacle Froude number rather than the obstacle height. Again, no steady-state first-order upstream disturbances were predicted. Baines (1977) attributed differences between experiment and theories of this type, of which McIntyre's is certainly the most well developed, to nonlinear finite-depth effects. There seems no doubt that a more sophisticated theory is needed to account for the upstream disturbances found in cases where the obstacle does not generate a significant separated wake. Since, in the limit of zero Froude number, the depth of blocked fluid must equal the body height, body lengthscales must presumably enter the theory explicitly.

In the case of obstacles generating an open separated turbulent wake, which Wei, Kao & Pao (1975) defined as 'source-like' but should perhaps be simply called 'more blunt', the situation seems rather different. These were perhaps the first authors to study the upstream columnar modes in any detail. Whilst for relatively streamlined bodies the first-order disturbances decayed with upstream distance and, with hindsight, could possibly have been similar to those studied by Baines (1979), for the more blunt obstacles steady-state first-order columnar modes like those in the Oseen theories were generated. However, no quantitative comparisons with theory were made.

McIntyre (1972) explicitly stated the likely difference between these two kinds of obstacles: 'in laboratory experiments, columnar disturbances could easily result from... drag associated with separation bubbles or local turbulent redistribution of x-momentum or buoyancy... these could correspond to the presence of forcing terms of type one' – i.e. giving disturbances of first order in h/D, rather than the second-order ones detailed in his theory. Snyder *et al.* (1985) have argued that many of the low-Froude-number towing-tank experiments on two-dimensional obstacles are misleading because steady-state conditions were never really achieved since the obstacles would probably, and in some cases demonstrably, have generated unattenuated first-order upstream disturbances.

The first objective of the present work was to obtain more detailed measurements of the upstream columnar modes than are available elsewhere and, in the absence of a suitable nonlinear theory, compare them with Oseen-theory predictions. Comparisons with the implications of the Foster & Saffman (1970) $F_h = 0$ results are included.

Many experimental studies have been concerned more with three-dimensional obstacles, since such cases generally have more direct relevance to atmospheric flows. Intuitively one might expect the upstream disturbances to become increasingly small as the spanwise width of the obstacle becomes smaller. Castro, Snyder & Marsh (1983, hereinafter denoted by CS) studied the stratified flow around the three-dimensional triangular ridges and found one or two puzzling features of the flow which, arguably, could have been caused by time-dependent upstream motions of sufficiently large amplitude to alter the upstream conditions. It is obviously important to have some 'feel' for the likely importance of upstream motions in such experiments; the second purpose of the current work was therefore to investigate upstream motions generated by three-dimensional obstacles.

This work has arisen from a wider study which included an investigation of the lee-wave field. The results of that aspect of the work have been reported separately (Castro 1987). We begin, in the following section, with a brief discussion of some of the relevant theories. The experimental techniques are described in §3 and the results are presented and discussed in §§4 and 5.

2. Upstream columnar waves, blocking and 'squashing'

We start by summarizing some of the well-known fundamental features of infinitesimal two-dimensional waves in a linearly stratified fluid. For horizontal wavenumber $k = 2\pi/\lambda$ (with λ equal to the wavelength) and circular frequency ω, the dispersion relationship for such waves is

$$\omega^2\left(k^2+\frac{n^2\pi^2}{D^2}\right)-N^2k^2 = 0.$$

Stationary waves are present if the obstacle speed is identical with the phase speed, i.e. if $F^2 = 1/(k^2D^2+n^2\pi^2)$ or $F < 1/n\pi$. (F is here based on channel depth D.) The group velocity of such waves is less than U so they appear only in the lee of the obstacle, but upstream-propagating waves with zero wavenumber and frequency will then also appear, since their group velocity, $ND/n\pi$, is greater than U. For $1/2\pi < F < 1/\pi$, only the lowest mode ($n = 1$) can propagate upstream; for $1/3\pi < F < 1/2\pi$, modes 1 and 2 can propagate upstream, and so on.

The wavelength of the lee waves follows directly from the above and is given by

$$\frac{\lambda}{h} = \frac{2\pi F_h}{(1-n^2\epsilon^2F_h^2)^{\frac{1}{2}}},$$

where F_h is the Froude number based on *obstacle* height and $\epsilon = \pi h/D$. CS showed that lee waves behind the obstacles used in the present experiment had wavelengths close to this 'two-dimensional limit' for the $n = 1$ mode, for all α (ratio of cross-wind length to height of the obstacle) and $F_h < 1$. The number of possible columnar modes, n_k, is $\mathrm{Int}(1/\epsilon F_h)$, where $\mathrm{Int}(x)$ denotes the integer part of x. $K = ND/\pi U = 1/(\epsilon F_h)$. As a typical example in the present study, with $\epsilon = 0.26$, $h = 9$ cm, and $F_h = 0.4$, nine modes are possible. The first mode travels the fastest, at a group velocity of ND/π or $U/\epsilon F_h$, i.e. about ten times the obstacle speed, with higher-order modes travelling progressively slower. Clearly if this $n = 1$ mode has any significant amplitude and can be reflected from the endwall without great attenuation, the obstacle cannot move very far down the tank before the flow around it begins to be affected by wave reflections. Indeed, *reflections* of the lowest-order waves may arrive at some distance upstream x, say, *before* the first arrival at x of the slower moving higher-order modes. The Oseen theories, which consider either a volume source or a momentum-sink-type disturbance, suggest that the amplitude of the columnar modes increases with mode number (see below), so that steady-state conditions at any particular x would not occur until *all* the wave modes had arrived at that position. In Baines' (1977) experiments, up to 11 modes were excited and the complicated structure of the upstream flow was evident. If reflections are suppressed (or the tank is long enough) it would presumably be possible in principle to achieve effectively steady-state conditions around the body itself once the slowest-moving upstream mode had moved far enough upstream to be out of the region in which the local pressure field of the obstacle was significant.

It is instructive to compare the basic results of Wong & Kao's (1970) and Janowitz's (1981, 1984) theories. The first authors assumed a volume source-like disturbance and it is easy to show from their results that the upstream columnar-mode velocity and density perturbations are given by

$$\frac{\Delta u}{U} = -\frac{Q}{UD}\sum_{n=0}^{n_k}\frac{K\cos(n\pi z/D)}{K-n} \qquad (1a)$$

$$\frac{\Delta\rho}{\rho_0} = \frac{NU}{g}\frac{Q}{UD}\sum_{n=0}^{n_k}\frac{K\sin(n\pi z/D)}{K-n}, \tag{1b}$$

where Q is the prescribed volume flux. Note that because of this flux, there is an $n = 0$ contribution to the velocity perturbation to satisfy continuity. Note also that although in many experiments NU/g is $O(10^{-2})$, this density perturbation is not small when compared with, say, the initial density difference over the obstacle height (e.g. $\Delta\rho/\Delta\rho_h$ is typically 0.4 in our experiments).

Janowitz (1981) used a momentum sink as the disturbance; for bounded obstacles this is perhaps more appropriate than a volume source. In his more recent generalization of the theory (1984) he showed that

$$\frac{\Delta u}{U} = -\gamma\sum_{n=0}^{n_k}\frac{n\cos(n\pi z/D)}{K-n} \tag{2a}$$

$$\frac{\Delta\rho}{\rho_0} = \frac{NU}{g}\gamma\sum_{n=0}^{n_k}\frac{n\sin(n\pi z/D)}{K-n}, \tag{2b}$$

where γ is the obstacle drag (made non-dimensional by $\rho_0 U^2 D$). There is an obvious similarity between (1) and (2), the major difference being that the higher-order waves are even more dominant in (2) than they are in (1), since n appears in the numerator. Wong & Kao assumed a source singularity, allowing Q to come outside the summation sign (i.e. $Q \neq f(n)$), but Janowitz noted that the force distribution G_n can be related directly to the drag by $G_n = 2n\pi\gamma$, provided that $n\pi b/D < 1$, where $b\ (< h)$ is the height of the streamline enclosing the force distribution, normalized by the tank depth. Now generally, $b = O(h)$, so that in the present experiments, taking $b = 0.5h$ as typical, the theory may only give reasonable results for $n < 8$. It can be shown that for higher-order modes, $G_n < 2n\pi\gamma$, so the relative amplitude of these modes may be rather lower than suggested by (2). The results presented later confirm that belief. Note that in common with all similar theories – and those based on Long's model – the solutions are singular for integral values of K.

It is also important to note that there is no body height scale (h, say) in these theoretical results so, as $F_h \to 0$, (1) and (2) do *not* give a superposition of higher and higher modes in a way that would lead to a fully blocked region of depth h extending upstream of the body. In fact, a Fourier superposition that did lead to such a region would require the wave amplitude to decrease with increasing wavenumber; (1) and (2) have the opposite behaviour. In this respect the theories are rather different from that of, say, Bretherton (1967) who studied inviscid inertial waves in a rotating fluid. (The body lengthscale was there included explicitly and the build-up of singularities at the edge of the Taylor column was shown to be associated with successive arrival of waves of smaller and smaller scale.)

It should be emphasized that these linear Oseen theories are, from a mathematical viewpoint, somewhat unsatisfactory. In addition to the obvious difficulty that first-order perturbations would seem to invalidate the Oseen approximation, Baines (1987) has argued that the generation of first-order disturbances must essentially be a nonlinear process, arising most clearly when K is closely integral (where linear theories break down). Whilst the columnar-mode propagation may be linear, it is therefore difficult to see how a linear theory could properly account for the *generation* of these modes. Grimshaw & Smyth (1986) have developed a non-linear theory (with h/D as the small parameter) for cases in which K is close to an integer but their results are not appropriate for the uniform-upstream-stratification case. As yet there

is no satisfactory nonlinear theory that can account for first-order disturbances. Despite these difficulties it is shown in this paper that the linear Oseen theories do seem to have some utilitarian value.

In the present experiments, the body shapes cannot be expected to lead to effective surface streamline shapes like those found by Janowitz (1981) for specific force distributions, but the relative amplitudes of different wave-mode velocity and density perturbations can still be usefully compared with the theories. Further, the density perturbations implied by (1) and (2) for a given Q or drag (deduced from the velocity perturbation results) can be compared with those expected from the 'squashing' model, to see how important wave reflections are in practice. Note that reflections cause velocity perturbations to cancel but density perturbations to accumulate. Foster & Saffman (1970) show that in the $F_h \to 0$ limit, the density perturbations are given by

$$\frac{\Delta\rho}{\rho_0} = \frac{N^2}{g}\frac{Ut}{L_1}z \quad \left(\text{for } \frac{z}{h} < 1\right),$$

where t is the time from the commencement of the tow and L_1 is the initial distance between the obstacle and the upstream endwall.

3. Apparatus and techniques

All the experiments were conducted in the large towing tank of the EPA Fluid Modeling Facility. Stratification of the nominally 1.1 m deep layer of water was achieved in the usual way with salt; Thompson & Snyder (1976) contains full details. As in CS an initially linear density profile with a nominal Brunt–Väisälä frequency of $N = 1.33\ \text{s}^{-1}$ was used and the upper few cm were syphoned off (with a corresponding layer of brine introduced at the bottom) after every few tows, to maintain the linear profile at the top.

Since we wanted to assess the possible influence of columnar motions on our earlier experimental results, most of the obstacles used were identical with those of CS, being 9 cm in height and triangular in cross-section, with flat vertical ends. Two additional obstacles, one with a 'Witch of Agnesi' shape (Baines 1977) and the other a simple (solid) fence, both of height 18.8 cm, were also used. The models were mounted upside down on a baseplate supported by a carriage, and towed at speeds ranging between about 1.2 and 12 cm/s. With a body height h of 9 cm and $N = 1.33\ \text{s}^{-1}$, this corresponds to $0.1 < F_h < 1.0$, but most of the measurements were made at $F_h = 0.2$ or 0.4. The baseplate extended upstream and downstream of the obstacles a distance of about $10h$ and $15h$, respectively (for $h = 9$ cm). It was fitted with a 5 mm diameter boundary-layer trip just downstream of the leading edge (to ensure similarity with our earlier experiments (CS) in which the intent was to minimize Reynolds-number effects), and was just submerged so that its surface was about 4 mm below the water surface. Figure 1 shows the general experimental set-up. The flow was illuminated by banks of fluorescent tubes mounted on one side of the tank, and cameras located on the opposite side and underneath were used to obtain permanent records of the flow structure. CS, Hunt & Snyder (1980) and Thompson & Snyder (1976) give complete details of these experimental arrangements.

The one new feature of our experimental techniques, not used quantitatively in any earlier experiments in the facility, was the method used to obtain velocity measurements within the developing upstream columnar-wave field. Prior to each

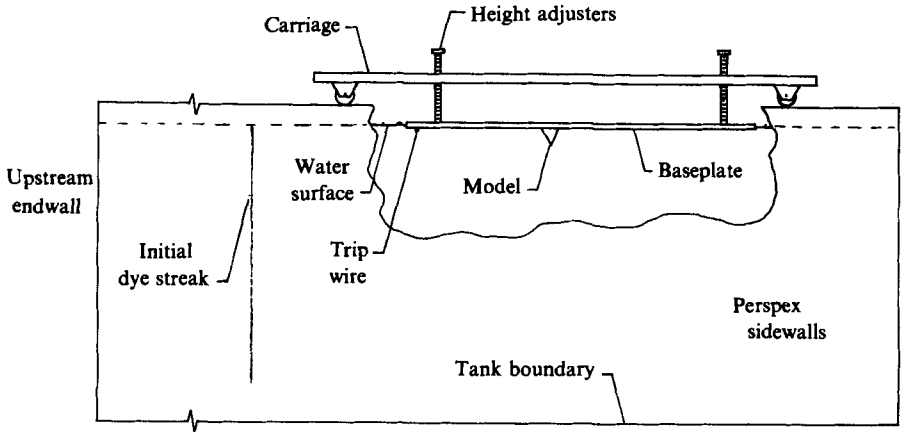

FIGURE 1. Experimental arrangement. Not to scale.

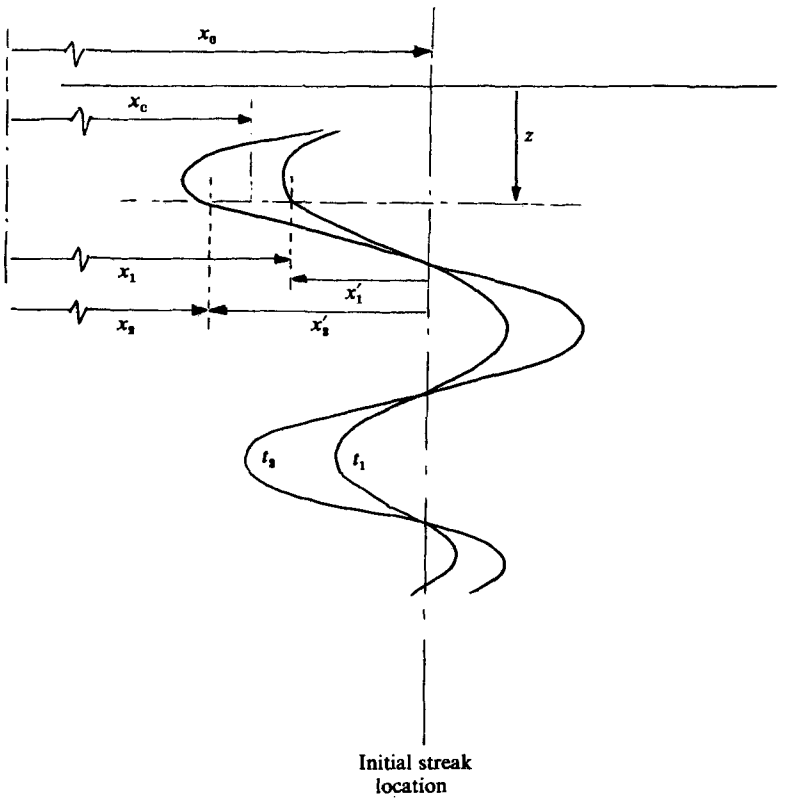

FIGURE 2. Dye-streak perturbations; explanatory sketch. See text for notation.

tow, vertical dye streaks at upstream locations equivalent to $x_0/h = 62$, 120 and 174 (at $t = 0$) were introduced by simply dropping a 'phial' of small potassium permanganate crystals into the tank, on the lateral centreline of the flow ($y = 0$). x is here measured positive upstream. Stationary cameras, mounted so that these streaks appeared centrally in their field of view, were then triggered automatically by the Facility's minicomputer, to take photographs at a sequence of preset times (not

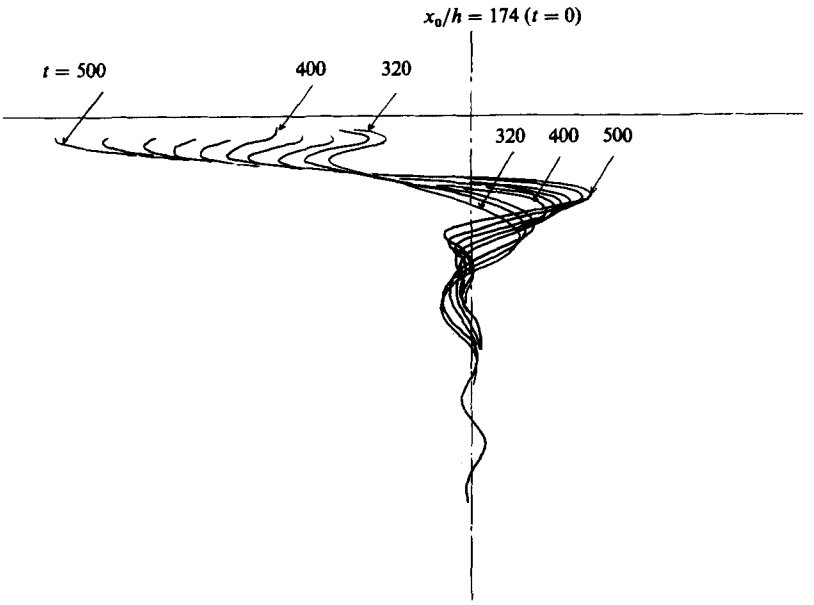

FIGURE 3. Actual streak perturbations for $\alpha = 2$, $F_h = 0.2$. From photographs taken 20 s apart at Frame 3. Elapsed time shown in seconds.

necessarily the same for each camera) after the start of the carriage. Upstream wave modes resulted in distortion of these streaks and, on the assumption that vertical motions are negligible, the horizontal velocity at any height and any time could be computed by comparing photographs taken just before and just after the required time.

The method actually used is best described with the aid of figure 2, which shows the shape of the dye streak after times t_1 and t_2. At $t = 0$, the streak is vertical and corresponds to a distance x_0 upstream of the starting position of the obstacle. Let the displacement of the streak from this line be x_1' and x_2' (at height z) after times t_1 and t_2. The velocity at a time $\frac{1}{2}(t_1+t_2)$ is then given by $(x_2'-x_1')/(t_2-t_1)$ and this occurs when the obstacle is a distance $x_0-U\frac{1}{2}(t_1+t_2)$ upstream of the vertical x_0 line. Strictly, the velocity so measured occurs when the body is a little closer than this, so all measurements included the appropriate correction to the obstacle location (x_c, in figure 2); this was only significant after long times when x_1' and x_2' could be large and the body was relatively close.

Scaling factors for the photographic prints were obtained by noting the positions of the obstacles in consecutive photographs and assuming that the development and printing process did not give variations within any one batch. Each tow resulted in up to 100 photographs, which were all processed together, and sets of traced dye streaks were obtained on the same sheet of paper by using a standard 'light box'. Great care was taken in ensuring that the paper was positioned as accurately as possible on each photograph, but inevitably the accuracy of the whole technique was probably no better than, typically, $\pm 5\%$ of the towing speed. The assumption of negligible vertical motion must clearly be inadequate in the vicinity of the body itself, although less so at the very lowest Froude numbers, so the accuracy deteriorates in that region.

Figure 3 shows a typical set of dye streaks, obtained for a case with $F_h = 0.2$, and

$\alpha = 0.2$, at 20 s intervals. It is clear that velocity estimates are most easily obtained near 'peaks and troughs' of the wave field, and that after long times the streaks can become so elongated that they disappear from the field of view entirely. Consequently, further dye streaks were frequently produced during the course of a tow by dropping in another phial of crystals. It should be noted that to obtain more resolution it is, in principle, only necessary to reduce the time between photographs. However, this eventually leads to more scatter in the calculated velocities, so that some compromise was often necessary; this amounted, in practice, to not always using the closest available streaks, at t_1 and t_2, to obtain the velocity at $\frac{1}{2}(t_1+t_2)$, but using instead streaks at $t_1-\Delta t$ and $t_2+\Delta t$.

Upstream density perturbations were obtained by drawing samples of fluid through vertical sampling rakes at various times and positions upstream. Because a finite time was required to obtain the samples, these were not truly instantaneous measurements, but the effects of finite sampling time are insignificant in the results presented here. Snyder *et al.* (1985) give full details of the technique and a few of our results were included in that work, but without any comparison with theory.

4. Two-dimensional cases

4.1. *Experimental results*

In this section experimental velocity and density perturbations upstream of the two-dimensional triangular ridges are presented; they are compared with the implications of the Janowitz (1984) and Foster & Saffman (1970) theories in §4.2. Recall that given a Froude number of $F_h = U/Nh$, modes 1 to n_k ($n_k = \mathrm{Int}(1/\epsilon F_h)$, with $\epsilon = \pi h/D$) will propagate upstream at speeds given by $ND/n\pi$. Mode n therefore arrives at a fixed upstream location x_0/h – measured from the initial obstacle location – after a time $(x_0/h)(n\pi/ND)$. It will subsequently be reflected from the upstream endwall of the tank after a time dependent on the initial position of the obstacle. Further reflections will occur at even greater times both from the endwalls of the tank and from the body itself if $z/h < 1$.

Figure 4(*a*) presents the variation with z/h of the perturbation velocity at $x/h \approx 16$, $F_h = 0.4$, deduced from photographs of the deforming dye streaks as explained in §3, for each of the three 'frames' (initial x_0/h locations). At this x/h, six, seven, and eight of the possible nine wave modes should have arrived at the first, second and third frames, respectively. It is clear that, as expected, higher wave modes influence the velocity profile at $x/h \approx 16$ as the obstacle moves farther down the tank, but the relative amplitudes of the different modes is less easy to discern. Qualitatively, it would seem that the amplitude increases with wavenumber, since at the last dye-streak position the velocity profile has a wavelength of around $3h$, or $0.25D$, corresponding to the eighth mode, whereas at the first frame the sixth mode is dominant. If the amplitudes of the higher modes were much less than those of the lower, the wave shape would be dominated by the lower modes.

The variation of amplitude with time at fixed z/h and each of the three dye positions is shown in figure 5, for $z/h = 1.5$, and in figure 6, for $z/h = 3.0$; the arrival times of the various modes and their reflections are also indicated. Note that since at the dye location farthest from the starting position (frame 3), the highest-order mode ($n = 9$) does not arrive until the body has approached to within about $13h$ of the initial streak location, a considerably longer tank would be required to ensure that the upstream flow in the vicinity of the body ($x/h < 20$, say) had reached steady state. Since the amplitudes of the upstream waves seem to increase with mode

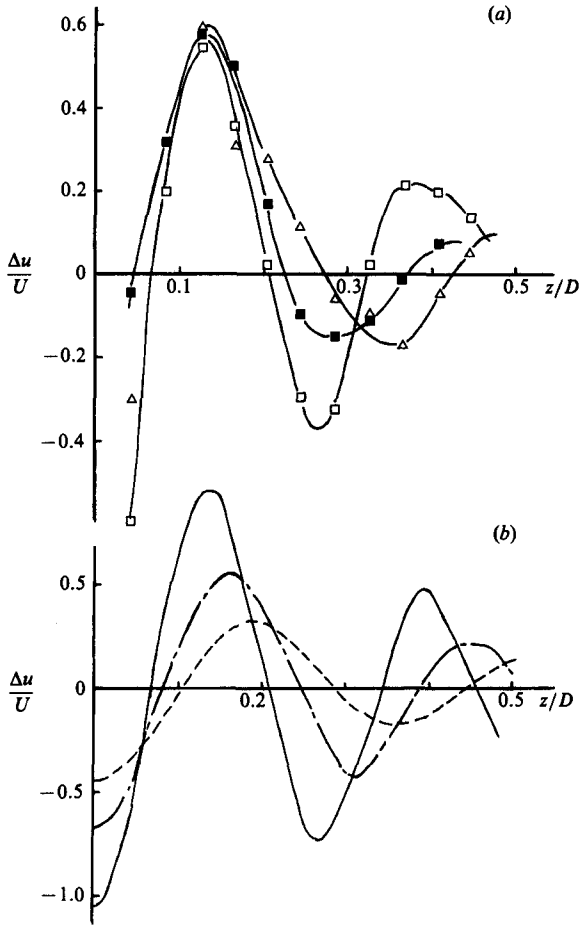

FIGURE 4. Velocity perturbations upstream of two-dimensional triangular ridge. $x/h = 16$, $F_h = 0.4$. (*a*) Data (frame, x_0/h): △ (1, 62); ■ (2, 120); □ (3, 174); lines added for clarity. (*b*) Janowitz (1984) theory, with $\gamma = 0.11$. x_0/h: ----, 62; ———, 120; ——, 174.

number, the most serious distortions of the upstream wave profile, caused by wave reflections, will presumably only occur once the slowest-moving (highest-order) wave reflections have arrived.

Some velocity perturbation measurements at a much lower Froude number were also made. Examples of these are presented in figure 7, which shows the results obtained at frame 3 ($x_0/h = 174$) after 170, 270 and 490 s from the start of the tow. Five, eight and fourteen modes should have arrived after these times, respectively; discussion is deferred to the following section.

Examples of the measurements of the upstream density perturbations are included in figures 8 and 9. In the former, the measured velocity and density perturbations at frame 2 ($x_0/h = 120$) after about 60 s are shown, when only the first three modes have passed and *no* reflections have yet arrived. At later times some reflections have arrived and figure 9 shows the velocity and density perturbations at frames 2 and 3 ($x_0/h = 120$ and 174) after times of 170 and 260 s, respectively. At these times the first seven modes should have arrived and, apart from the probably small influence of viscosity and diffusivity, the only mechanism that can lead to different wave

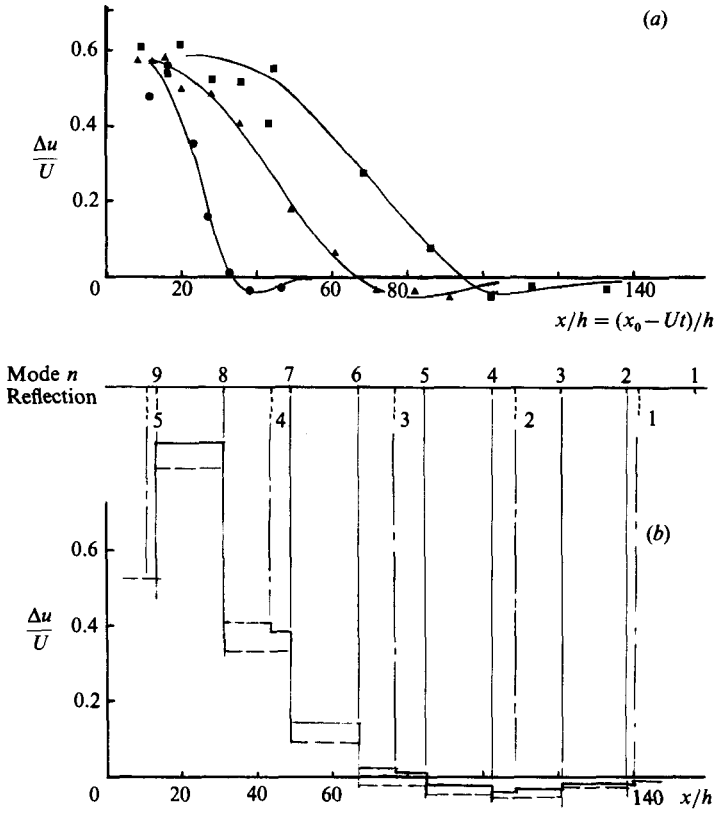

FIGURE 5. Velocity perturbations at fixed positions in the tank as functions of time. $F_h = 0.4$, $z/h = 1.5$ ($z/D = 0.125$). (*a*) ●, Data for frame 1; ▲, 2; ■, 3. Lines added for clarity. (*b*) Janowitz's theory for frame 3 with $\gamma = 0.11$; dashed lines are results without reflections. Arrival times of each mode (and its first reflection) at frame 3 are indicated.

shapes at the two frames is reflections from the endwalls and the body itself – different numbers of reflected modes having arrived at each frame. In this case, reflections of the first four modes should have reached the third frame, compared with only the first two modes at the second frame.

Although the density perturbations are relatively small, they constitute large local variations in the Brunt–Väisälä frequency. For example, around $z/h = 2$, the change in N from its initial value of 1.33 s^{-1} is about 0.8 s^{-1}. After eventual arrival of the two highest-order modes in this case ($n = 8, 9$), the change would be even greater so, even without reflections, the final steady-state upstream conditions (after arrival of all the modes) would be very different from the initial conditions. Indeed, after the seventh mode has arrived, the local Richardson number, $Ri = h/U^2\, \mathrm{d}\rho/\mathrm{d}z$, varies by almost an order of magnitude between $0.0 < z/h < 2.5$. The largest changes occur near $z = 0$ – in this case, at $z = 0$, Ri is about 60 compared with the initial value of 6.25.

More extreme cases are presented in figure 10, which shows some density perturbations measured just 1 m from the upstream endwall of the tank. In this case, two different models were used: a simple vertical fence and a 'Witch of Agnesi'-shaped hill, both 18.8 cm in height. The model Froude number was 0.21 in both cases and results at 122, 245 and 367 s are shown.

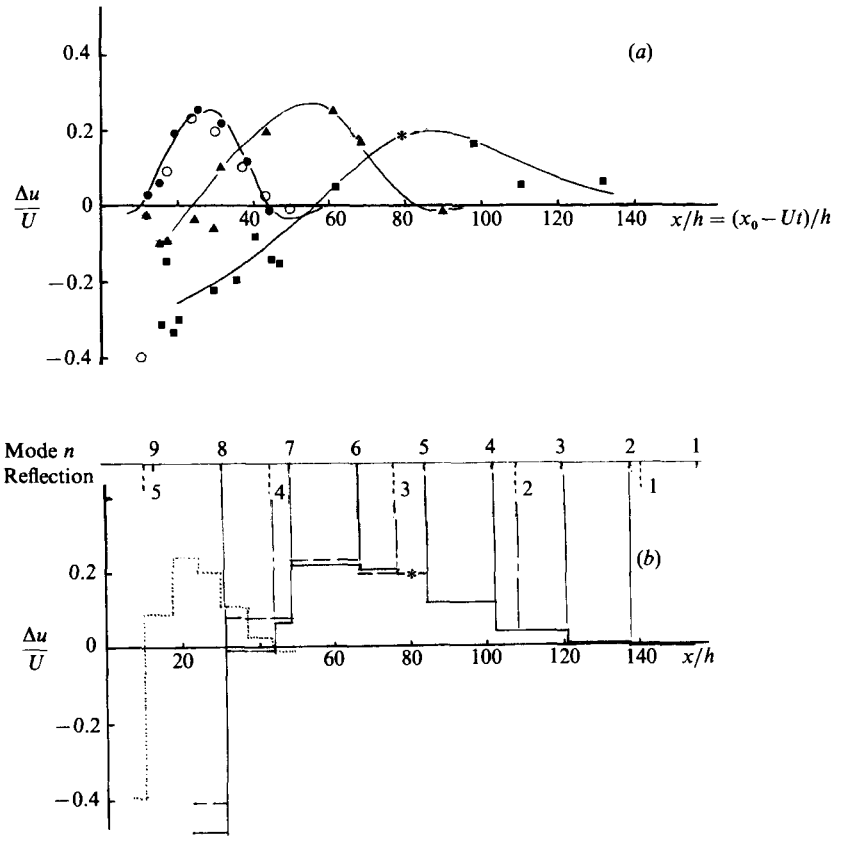

FIGURE 6. As for figure 5, but at $z/h = 3.0$ ($z/D = 0.25$). In (b) the dotted line is for frame 1 – the open circles in (a) correspond to it; * is the matching point giving $\gamma = 0.11$.

4.2. *Comparisons with theory*

Figure 4(b) shows the expected wave shapes according to the theory of Janowitz (1984) (equation 2a); the drag γ was taken as 0.11 (see below). The calculations include the effect of perfect wave reflections from the upstream endwall, but this makes little difference because only the first few (and weakest) reflected modes had arrived at frames 2 and 3 by this time. Wong & Kao's (1970) results would be very similar except for a rather smaller change in relative amplitudes between modes. It is evident that the wave shapes are roughly in accordance with the predictions, but the experiments show a rather weaker amplitude variation between modes than is indicated by the theory. It should be noted, however, that these data are all for $x/h = 16$, which may be sufficiently close to the body to be within the region affected by the additional upstream perturbations which decay quite rapidly with x (Wong & Kao 1970; Janowitz 1981).

Figures 5(b) and 6(b) show the theoretical changes in wave amplitude at a fixed z/h that occur when the various modes arrive. In the absence of viscosity, the arrival of each mode would lead to a step change in velocity. In practice, of course, one would not expect abrupt changes in wave amplitude at these times; the individual modes will not reach their full strength at the mode crossing time. One immediate deduction is that, again, the general theoretical result of wave amplitude increasing

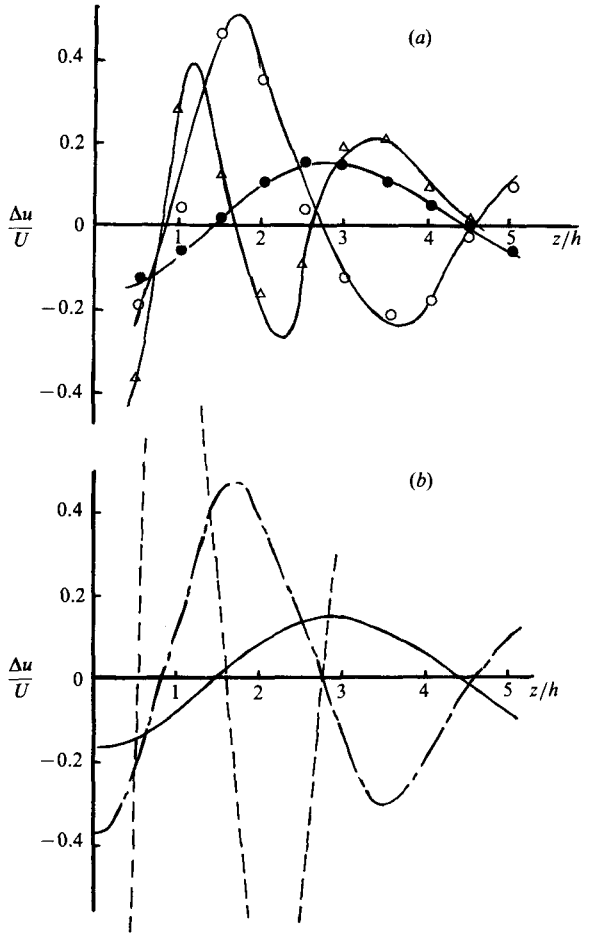

FIGURE 7. Velocity perturbations upstream of two-dimensional ridge. Frame 3 ($\alpha = \infty$), $F_h = 0.18$. (*a*) ●, Data after $t = 170$ *s*; ○, 270 s; △, 490 s; lines added for clarity (*b*) ——, Theory with $\gamma = 0.26$ after $t = 170$ s; – – – –, 270 s; – – –, 490 s.

with mode number is consistent with the data except, as expected, for the highest wavenumbers, when the experimental amplitudes are rather lower. It is worth noting, however, that the qualitative trend in the evolving wave shape is not too dependent on the way in which wave amplitude varies with wavenumber. Only if the amplitude *decreased* fairly rapidly with wavenumber would the theoretical results look significantly different from the data of figures 5(*a*) and 6(*a*). Figures 5(*b*) and 6(*b*) also show the Janowitz (1984) results without inclusion of the reflections, for the third frame position only. At this position, only the first four reflected modes arrive before the body is within $x/h = 12$ of the initial dye-streak position, and reflections do not appear to alter seriously the wave field prior to this.

The theoretical wave amplitudes shown in figures 4, 5 and 6 were obtained by matching the result for the sum of the first five modes (at $z/h = 3$, figure 6) with the experimental value at $x/h = 80$ and frame 3. This implied a value of about 0.11 for γ, corresponding to a drag coefficient of about 1.3 based on the body height. This was used to obtain all the other theoretical results shown in these figures. Slightly different values of γ would be obtained if the matching were performed at different

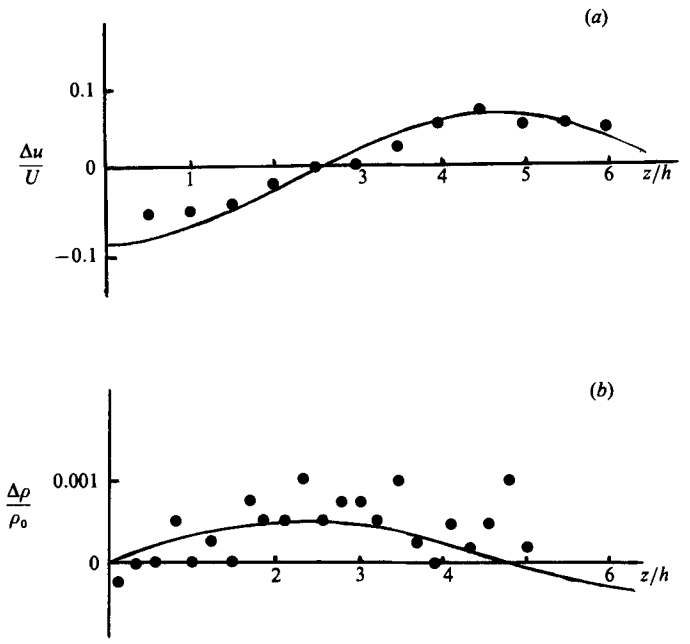

FIGURE 8. Velocity (*a*) and density (*b*) perturbations at frame 2 after 60 s. ●, data; ——, theory with $\gamma = 0.11$ ($F_h = 0.4$).

spatial or temporal positions, but the general level of agreement between the theoretical and experimental results would not be significantly affected.

With the value of γ deduced from the velocity data it was possible to compare the density perturbations with those expected on the basis of the theory. The theoretical results are included in figures 8 and 9. In the latter case perfect reflections of the first two and the first four modes (from the endwalls only) have been assumed whereas in the former case no reflections are included – see §4.1. Note that the inclusion of reflections from the body itself rather than the downstream endwall, for $z/h < 1$, would make little difference to the theoretical results.

In all cases the experimental density perturbations have about the magnitude expected on the basis of the Janowitz (1984) theory. It should be emphasized that the $\Delta\rho/\rho_0$ data were obtained as a difference between two density-profile measurements, so that there is inevitably some scatter – the maximum perturbation is only about 0.5%! In the cases where some reflections are expected to have arrived (figure 9) the density data also follow at least qualitatively the expected differences in perturbation profiles at the two frames, caused by differences in the number of reflected modes. The velocity data are not quite so consistent: for $z/h > 3.0$ the frame-2 perturbation velocity seems rather more positive than expected.

Viewing all these figures (5, 6, 8, 9) as a whole, it is evident that the theory of Janowitz (1984) not only gives a good qualitative description of the upstream flow but also provides reasonable quantitative estimates for the magnitude of the velocity and density perturbations, provided a suitable value for the drag is chosen. The figure 4 data are probably, as indicated earlier, influenced by attenuated waves in the region near the obstacle. Now these data are all for $F_h = 0.4$ and $\pi h/D = 0.26$, for which a maximum of nine wave modes are excited. As noted in §2, the theory is only valid for $n\pi b/D > 1$, where b is the effective height of the force distribution at

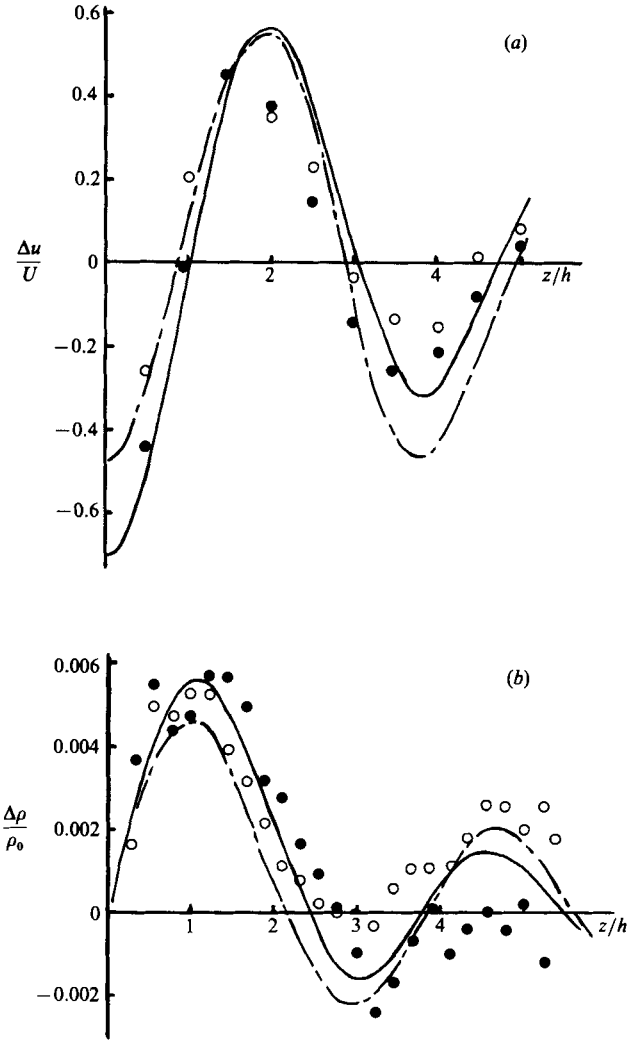

FIGURE 9. Velocity (*a*) and density (*b*) perturbations ($\alpha = \infty$) at $F_h = 0.4$. (frame, t): ● (3, 260 s); ○ (2, 170 s). ——, Theory with four reflections; – – – –, theory with two reflections.

$x = 0$. Taking $b = \frac{1}{2}h$, all wave modes (except possibly the ninth) satisfy this condition. The experimental data are consistent with that. However, at lower internal Froude numbers, higher-order wave modes will travel upstream and the amplitude of these will presumably not be adequately described by the theory since they will not satisfy the above condition. Our experiments at $F_h = 0.18$ seem to demonstrate this. Figure 7(*b*) shows the theoretical velocity perturbations at frame 3 ($x_0/h = 174$), obtained by matching the peak positive velocity perturbation obtained at $t = 170$ s. This implies a drag coefficient γ of about 0.26. All reflections from both endwalls have been taken into account. The $t = 270$ s data are wholly consistent with the theory, but the amplitude (though not the wavelength) of the $t = 490$ s profile, after fourteen modes should have arrived, is very much smaller than the theoretical result. Similar data for lower values of x_0 (frames and 1 and 2) have the same characteristics, being consistent with the theory (with $\gamma = 0.26$) only up to

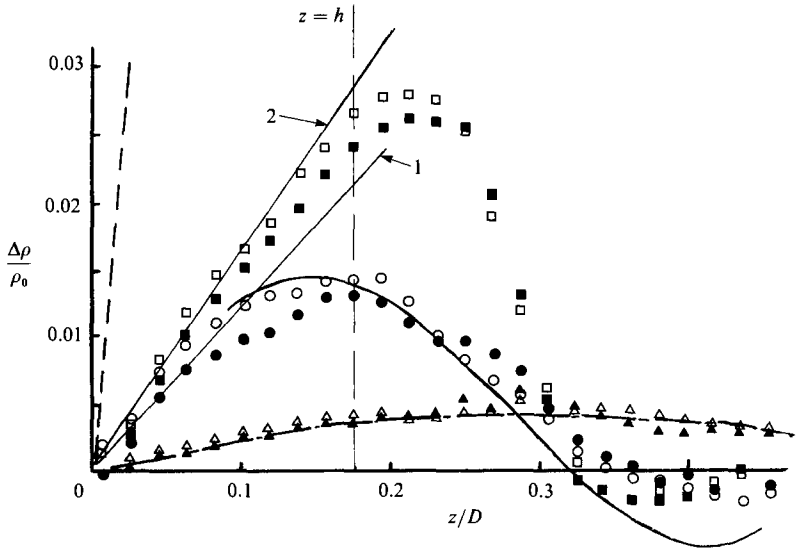

FIGURE 10. Density perturbations 1 m from upstream endwall after $t =$: ▲, 120 s; ●, 245 s; ■, 367 s; $F_h = 0.21$. Closed symbols, 'Agnesi' hill; open symbols, fence. ———, Theory after $t = 120$ s; ——, 245 s; – – –, 367 s. Lines 1 and 2 are the Foster & Saffman predictions for $t = 245$ s and 367 s respectively.

the arrival of the first eight or nine modes. Evidently the amplitudes of the higher-order modes do not continue to rise so rapidly with wavenumber and, as expected, the theory breaks down for $n\pi b/D > 1$.

A further indication of this behaviour is apparent from the density results in figure 10. Included in the figure are the density variations calculated using the Janowitz (1984) theory, matching the peak $\Delta\rho/\rho_0$ values after 122 s, by which time only the first two modes have arrived. After 245 s the first five modes should have arrived, although the fifth only arrives a little before 245 s and will presumably not have reached its full strength. Since the density profiles were obtained during a period of about 20 s, the theoretical result for just the first four modes (plus any reflections) is shown. The data are consistent with this result. However, although by 367 s at least seven (of the maximum nine) modes should have arrived, the data do not show much further change in wavelength and, furthermore, the amplitudes are very much less than those obtained from the theory. The latter are so large that they cannot even be included on the same graph, but the variation near $z = 0$ is shown. In this case $n\pi b/D < 1$ is satisfied by only the first four modes so, again, the data seem to confirm the adequacy of the theory, provided this criterion is satisfied, and imply considerably lower amplitudes for the higher-wavenumber modes which do not satisfy $n\pi b/D < 1$.

Since these higher-wavenumber modes seem to be relatively insignificant, it is reasonable to suppose that the perturbation profiles might be similar to those expected on the basis of the Foster & Saffman (1970) theory, valid for $F_h = 0$. These are included in figure 10. Now the theory was for $F_h = 0$ so that all (infinite) wave modes have a group velocity infinitely larger than the obstacle speed, leading to simultaneous arrival of all modes plus their reflections. In practice of course, for $F_h < 1$ the 'squashing' mode perturbations develop only after the finite time required for arrival of all significant modes and grow with time as a result of a rapidly

increasing number of reflections between the obstacle and the endwall as the latter is approached. It is interesting that, in figure 10, arrival of the first four modes (by $t = 245$ s) leads to a perturbation density gradient near $z = 0$ very close to the Foster & Saffman prediction; thereafter the profile changes, presumably because of the addition of further reflections. Actually calculations show that the linear addition of further reflections between the *obstacle* and the upstream endwall for increasing time (using just the first four modes) gives amplitudes at $t = 367$ s a little in excess of the data and the Foster & Saffman result. These are not shown, however, since it is most unlikely that linear theory could describe in detail the final transition between the behaviour before reflections become significant and that in the last part of the tow when they must become dominant for $F_h < 1$.

As a final comment on figure 10, it is significant that there is so little difference between the results for the fence and the 'Agnesi' hill. At higher Froude numbers we expect the wave amplitudes to be dependent on the obstacle drag so, given that the same drag for these two obstacles seems at first sight highly unlikely, a possible implication of the data is that $F_h = 0.2$ is sufficiently close to the $F_h = 0$ limit to make the obstacle shape (other than height) of only secondary importance: wave drag is clearly irrelevant at $F_h = 0$ and the viscous drag in the shear layer at $z = h$ will presumably be independent of the body shape. On the other hand G. S. Janowitz (private communication) has suggested that for obstacles sufficiently short even the wave drag may not be a strong function of body shape. Proper confirmation of this assertion would not be easy, but if $F_h = 0.2$ is considered to satisfy $F_h \gg 0$, the data shown in figure 10 are not inconsistent with the idea.

5. Three-dimensional cases

Although a number of velocity-perturbation measurements were made for cases of three-dimensional triangular ridges, there were various confusing aspects of the results; we shall therefore not present them here in detail, although some comments are appropriate. Whilst the columnar modes were in all cases clearly weaker than those found for two-dimensional obstacles, they led to changes in upstream velocity conditions that were certainly measurable. One might expect that the lowest-aspect-ratio obstacle ($\alpha = 2$) would generate weaker upstream waves than the highest ($\alpha = 8$); the results had a slight trend in that direction. Some tows were made with the baseplate alone and also with the obstacle alone (no baseplate). In the former case the results were very similar to the $\alpha = 2$ data. Without the baseplate the $\alpha = 2$ data lay scattered about $u = 0$ whereas for $\alpha = 8$ perturbations were clearly significant. Evidently the baseplate itself, which was submerged by typically 4–5 mm and had a 5 mm trip wire mounted near its leading edge, was the dominant cause of the upstream disturbances in the runs made with the smaller three-dimensional obstacles. This result serves as a warning for any future planning of similar experiments.

Data were also obtained from a tow of a circular hill of height 15.5 cm, whose shape was defined by $h(r) = H/(1+(r/L)^4)$, with L, the radius at which $h = \frac{1}{2}H$, of 39 cm. The internal Froude number (U/ND) was the same as in the other cases; this ensured that the same number of wave modes (9) were excited. The data showed that the wave amplitudes were considerably greater than those generated by the triangular ridges, lying roughly half-way between the $\alpha = 8$ and $\alpha = \infty$ data. Since the projected frontal area of this hill was some two to three times as great as that of the $\alpha = 8$ triangular ridge this was, perhaps, not surprising.

There was no doubt that the upsteam columnar disturbances in the three-dimensional cases followed the general pattern of the two-dimensional results but for small obstacles could be dominated by the motions generated by the baseplate itself. The practical implication of these results for the associated work described by CS and Castro (1987) is that since, for $F_h > 0.4$ at least, the highest-order modes had arrived at the third dye-streak position (which is where the lee-wave photographs were generally taken) by the time the body had approached to within $x/h = 13$ of that position, we are confident that the lee-wave fields observed for the $\alpha < 8$ cases had reached their steady-state configurations: the perturbations do not have disturbingly large amplitudes. This was not necessarily the case for the wider bodies ($\alpha > 8$); certainly any rotors generally seemed to take longer to develop in these cases (Castro 1987). However, the results for the circular hill, in particular, imply that even in the case of three-dimensional obstacles great care must be exercised in planning experiments if steady-state upstream conditions are sought.

Finally, some density perturbations upstream of the circular hill were also measured and these were not inconsistent with the Janowitz theory if a drag obtained by matching the velocity data were used. The results confirmed that the influence of endwall reflections (squashing) was insignificant in our three-dimensional experiments. It does not seem profitable to make detailed comparisons between these three-dimensional experiments and two-dimensional theory. The perturbations must decay with distance upstream, for they can spread laterally, but we have not made a thorough study of that aspect of the problem. In view of its practical importance for three-dimensional experiments, it may well be worth further investigation.

6. Conclusions

The basic conclusions of the present work can be summarized as follows.

(i) In two-dimensional towing-tank experiments in which $ND/\pi U > 1$ the columnar modes propagating upstream of the towed obstacle can have significant amplitudes. Unless the obstacle height parameter, h/D, is very small and the obstacle has an 'easy' shape, the perturbations are of first order and therefore of different type from the second-order perturbations described by theories like those of McIntyre (1972) or Baines & Grimshaw (1979). The non-decaying large-amplitude disturbances found in the present work were similar to those described by Wei *et al.* (1976) for obstacles generating an open, turbulent separated wake.

(ii) The theoretical results of Wong & Kao (1970) and Janowitz (1981, 1984) describe qualitatively the form of the upstream perturbation velocity and density profiles. Further, our experiments show that Janowitz's theory gives a reasonable quantitative indication of the relative amplitudes of the different modes (for multiply subcritical cases) provided $n\pi b/D < 1$, with $b/h = 0.5$. In this range the wave amplitude increases with wavenumber, although the rate of increase is possibly rather lower than that predicted by the theory and, in any case, the higher-wavenumber modes (for which $n\pi b/D > 1$) have less significant amplitudes. Taking, say, ten body heights to be a measure of the upstream distance beyond which the obstacle's pressure field becomes insignificant, the implication of these conclusions is that steady-state upstream conditions cannot practically be achieved, even ignoring endwall reflections, until the highest wave mode has arrived at $x/h = 10$. If $K = ND/\pi U$ is only slightly larger than an integral value, the highest-order wave travels upstream at a relative speed very slow compared with the body speed, so the

body may have to travel a distance of at least $O(100h)$ before this wave arrives at $x/h = 10$. If the wave amplitudes had been found to decrease with wavenumber (contrary to the Janowitz theory) then roughly steady-state conditions would have been achieved earlier.

(iii) In cases where the Froude number is so small that the higher-order modes have $n\pi b/D > 1$, steady-state conditions may be achieved rather earlier than anticipated on the basis of the speed of these modes, since their amplitude is relatively insignificant. The Foster & Saffman (1970) $F_h = 0$ theory provides an upper limit on the rate at which the density perturbations grow in the $z/h < 1$ region and, for $F_h = O(\frac{1}{10})$ experiments, provides reasonable quantitative estimates of the upstream density perturbations, independent of the obstacle drag.

(iv) The density perturbations $(\Delta\rho/\rho_0)$ caused by the columnar modes have typical amplitudes of order NU/g times those of the velocity perturbations. In our experiments, $NU/g \approx O(10^{-2})$ but it is more appropriate to compare the density perturbations with the initial density difference over the body height; together with the velocity perturbations these density changes imply substantial perturbations in local Richardson number.

(v) In experiments with three-dimensional obstacles upstream perturbations are relatively small unless the obstacle spanwise width is a large fraction of the tank width. In the present work, for the smallest obstacles, the perturbations appeared to be caused largely by the (small) submersion of the baseplate and the presence of a substantial leading-edge trip wire. Together, these 'two-dimensional objects' generated motions very similar to those found in the true two-dimensional-hill experiments, though of rather lower amplitude. In any future investigations of the upstream decay of the columnar modes in three-dimensional cases, care will be needed to ensure that the generated upstream motions are a result solely of the obstacle. For significantly larger obstacles, more significant velocity and density perturbations were observed, but in no case were the effects of endwall reflections and squashing noticeable.

The three-dimensional results also indicated a slight trend of increasing wave amplitudes with increasing obstacle spanwise aspect ratio, as might be intuitively expected. We do not believe that the amplitudes were sufficiently high to influence the major conclusions of our previous experiments (e.g. Hunt & Snyder 1980; Castro *et al.* 1983; Castro 1987) but they could perhaps have been reduced further by minimizing the baseplate submersion.

The fact that a linear theory apparently does so well in predicting the upstream disturbances for cases that would normally be considered strongly nonlinear is perhaps the most surprising feature of our results. It should be emphasized, however, that the obstacle drag is not predicted by the theory; choosing a suitable value merely makes our data on the relative strengths of the different modes consistent with the theoretical results. Presumably more appropriate theories yet to be developed would not lead to large quantitative changes in these relative mode strengths. However, further careful experiments of this sort with different types of obstacle would undoubtedly be helpful in elucidating the range of validity of the various theories.

This work has benefited from many discussions with the authors' colleagues at the Fluid Modeling Facility. We are grateful, in particular, to Dr R. E. Eskridge, Mr R. S. Thompson and Mr R. E. Lawson, but thanks are also due to the entire staff at

the Facility. The comments of Dr J. Rottman and the referees on earlier versions of this paper were also very helpful. I.P.C. acknowledges support from North Carolina State University as a Visiting Associate Professor under a Cooperative Agreement (No. 807854) with the US Environmental Protection Agency.

REFERENCES

BAINES, P. G. 1977 Upstream influence and Long's model in stratified flows. *J. Fluid Mech.* **82**, 147–159.

BAINES, P. G. 1979 Observations of stratified flow over two-dimensional obstacles. *Tellus* **31**, 351–371.

BAINES, P. G. 1987 Upstream blocking and airflow over mountains. *Ann. Rev. Fluid Mech.* **19**, 75–97.

BAINES, P. G. & GRIMSHAW, R. H. J. 1979 Stratified flow over finite obstacles with weak stratification. *Geophys. Astrophys. Fluid Dyn.* **13**, 317.

BRETHERTON, F. P. 1967 The time-dependent motion due to a cylinder moving in an unbounded rotating or stratified fluid. *J. Fluid Mech.* **28**, 545–570.

CASTRO, I. P. 1987 Further measurements of the lee-wave structure in stratifield flow over three-dimensional obstacles. *Tellus* **39A**, 72–81.

CASTRO, I. P., SNYDER, W. H. & MARSH, G. L. 1983 Stratifield flow over three-dimensional ridges. *J. Fluid Mech.* **135**, 261–282.

FOSTER, M. R. & SAFFMAN, P. G. 1970 The drag of a body moving transversely in a confined stratified fluid. *J. Fluid Mech.* **43**, 407–418.

GRIMSHAW, R. H. J. & SMYTH, N. 1986 Resonant flow of a stratified fluid over topography. *J. Fluid Mech.* **169**, 429–464.

HUNT, J. C. R. & SNYDER, W. H. 1980 Experiments on stably and neutrally stratified flow over a model three-dimensional hill. *J. Fluid Mech.* **96**, 671–704.

JANOWITZ, G. S. 1968 On wakes in stratified fluids. *J. Fluid Mech.* **33**, 417–432.

JANOWITZ, G. S. 1981 Stratified flow over a bounded obstacle in a channel of finite depth. *J. Fluid Mech.* **110**, 161–170.

JANOWITIZ, G. S. 1984 Upstream disturbances in stratified channel flow. Unpublished Rep., Dept. Marine, Earth and Atmospheric Sciences, N.C. State Univ., Raleigh, NC 27650.

LONG, R. R. 1953 Some aspects of the flow of stratified fluids. I. A. Theoretical investigation. *Tellus* **5**, 42–57.

LONG, R. R. 1955 Some aspects of the flow of stratified fluids. III. Continuous density gradients. *Tellus* **7**, 342–357.

MCINTYRE, M. E. 1972 On Long's hypothesis of no upstream influence in uniformly stratified or rotating fluid. *J. Fluid Mech.* **52**, 209–243.

SNYDER, W. H., THOMPSON, R. G., ESKRIDGE, R. E., LAWSON, R. E., CASTRO, I. P., LEE, J. T., HUNT, J. C. R. & OGAWA, Y. 1985 The structure of strongly stratified flow over hills: dividing streamline concept. *J. Fluid Mech.* **152**, 249–277.

THOMPSON, R. S. & SNYDER, W. H. 1976 EPA Fluid Modeling Facility. In *Proc. Conf. on Modeling and Simulation, Rep.* EPA-600/9-76-016. Washington D.C.: Environment Protection Agency.

TRITTON, D. 1977 *Physical Fluid Dynamics.* Van Nostrand Reinhold, 362 pp.

TRUSTRUM, K. 1964 Rotating and stratified fluid flow. *J. Fluid Mech.* **19**, 415–432.

TRUSTRUM, K. 1971 An Oseen model of two-dimensional flow of a stratified fluid over an obstacle. *J. Fluid Mech.* **50**, 177.

WEI, S. N., KAO, T. W. & PAO, H. P. 1975 Experimental study of upstream influence in the two-dimensional flow of a stratified fluid over an obstacle. *Geophys. Fluid Dyn.* **6**, 315–336.

WONG, K. K. & KAO, T. W. 1970 Stratified flow over extended obstacles and its application to topographical effects in vertical wind shear. *J. Atmos. Sci.* **27**, 884–889.